

# CALIBRATION AND NAVIGATION OF A TRANSRECTAL ULTRASOUND PROBE FOR PROSTATE CANCER THERAPY

D. Richter\*, H. Voss\*, K. Berthold\* and G. Straßmann\*\*

\* Department of Computer Science, University of Applied Sciences of Wiesbaden, Germany

\*\* Department of Radio-Oncology, University of Marburg, Germany

richter@informatik.fh-wiesbaden.de

**Abstract:** An infrared light based stereoptical navigation system and a 3-D-calibration pattern are used to calibrate a transrectal ultrasound probe for interstitial brachytherapy. The intersection points of the US image with a 3-D-calibration pattern are interactively defined. These points define the position of the US image with respect to the calibration device. The relative positions of the US probe and the calibration pattern are measured with the navigation system. Hence the coordinates of the US image can be transferred into the probe coordinate system and into a world coordinate system. The calibration procedure and measurements are given in detail. The tilt and slant of the US image are in the order of one degree. To use US imaging for precise biopsy needle navigation the accurate position of the image has to be considered.

## Introduction

In the case of interstitial brachytherapy for prostate cancer steel needles are applied with a template grid placed in front of the perineum due to the preplanning of an irradiation program under control of US imaging. The grid holes have distances of 5 mm in both spatial directions. The procedure implies inaccuracies of up to 5 mm with respect to the prostate and constrains the needles to parallel paths. To avoid these constraints and to improve irradiation accuracy an IR-based stereoptical 3-D-navigation system is under development [1], which in future will also allow oblique needle paths to be applied under control of ultrasound images using a needle tracking system. Therefore a calibration procedure to define the exact image plane of the transrectal ultrasound (TRUS) probe has to be developed. The calibration procedure is also based on the 3-D-navigation system.

## Specifications and Requirements

The ultrasound scanner used is a Falcon EXL type 2101 with a TRUS probe type 8658 ( B-K Medical, Herlev, Denmark ). The ultrasound images which are displayed on the monitor of the ultrasound scanner are digitised by a framegrabber board DT 3152 (Data Translation GmbH) to which the scanner is connected via a coaxial cable.

To determine the spatial position of the TRUS probe for navigation three IR-LEDs are mounted on the

probe. As described in [2,3], infrared light emitting diodes (IR-LEDs) with flat milled heads are used as landmarks of the probe. These purpose-built IR-LEDs have a light-emitting angle of 70° in contrast to 17° of conventional ones. This allows the detection of their emitted light at greater angles. They are mounted in a shape closely resembling an acute-angled isosceles triangle. This leaves it to the software to decide the direction of the triangle. The three diodes span a plane which defines the  $x_p, y_p$ -plane of the probe coordinate system. Since the probe is not turned around the longitudinal axis of more than 90° and the IR-LEDs are only emitting light to the upper side, the rotational symmetry is unambiguous. One of the IR-LEDs is mounted behind the probe handle, the other two in front. Since this is the longest possible distance to arrange the diodes, the error of measuring the angle in the probe's direction is minimized.

Two 1/2" CCD chip monochrome video cameras, type Teli CS8320 BC are used to take images of the scene. They operate at 50Hz interlaced mode, resulting in 25 video frames per second. The video images have a resolution of 752 x 576 pixel with 8-bit grey levels. The analogue VB signals are transferred to two Data Translation DT3152 frame grabber boards via coaxial cables. The cameras are externally synchronized. In front of the objectives (12.5mm focal length) the cameras are equipped with Schott long pass glass filters type RG830 with cut-off frequency of 830 nm.

The cameras are mounted above the TRUS probe, which is placed in front of the rectum. For the used stereo base of approx. 104 cm and a height over the calibration pattern of approx. 140 cm, the cameras are mounted at an angle of 18° in this position. Thus a field of about 68 x 54 cm<sup>2</sup> of the calibration table is visible to each camera.

For the probe calibration a calibration device was used. It forms a 3-D N-shaped pattern of nylon strings, which are clamped in different heights between two acrylic plates, as it is used by different groups for calibration purpose [4,5,6]. At the top of the calibration device three IR-LEDs of the same type as the probe are mounted. The intersection of the US image with the 3-D pattern is used for calibration.

Since the impedance of US in air is very high, the calibration is done in a water basin which is common practice. The side wall of a water basin was provided with a TRUS probe inlet and sealed with an O-ring

flange. Thus the probe can be laterally inserted into the basin.

The IR-LEDs of both the TRUS probe and the calibration device are connected to a power supply via an electronic switch, which is connected to the PC via the USB port. Thus the LEDs can be switched on or off by the developed application depending on the program in use.

### Procedure

To define the intrinsic and extrinsic camera parameters the cameras are modelled as pinhole cameras with radial symmetric distortions of the optical lenses. A chessboard-like pattern is used for a Tsai-based [7,8] single-plane calibration. The cameras of the stereo-optical system are synchronized to ensure a simultaneous image acquisition. The IR-LEDs of the TRUS probe in the images are segmented and their 3-D position and orientation in space calculated. IR-LEDs in camera images are not shown as points at one single pixel position, but as nearly round gray value fields with a diameter of about 10 pixels. The weighted center of the gray value pixels is calculated and set as pixel coordinates for the specific diode. Because of the ambiguous correlation of corresponding points in both camera images, all 9 combinations of the diode coordinates are calculated as 3-D points in the world coordinate system  $C_w$ . Their mutual distances are calculated and compared to the diode distances of the defined LED geometry model. The exact model is calculated with the help of the system by measuring the LED positions in an arbitrary position of the probe using the approximate distances of the LEDs to initially solve the correspondence problem. An average out of 100 measurements is used for defining the geometry model.

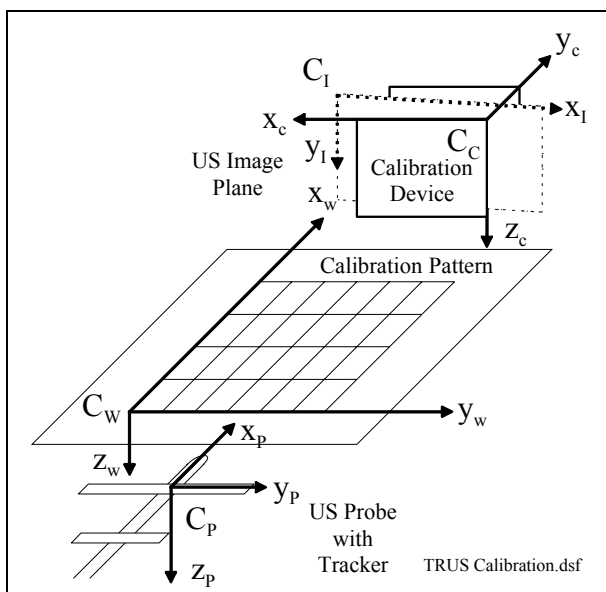


Figure 1: Definition of the coordinate systems  $C_p$ ,  $C_w$ ,  $C_c$  and  $C_1$ .

The three diode positions with the best matching of a rigid transformation between the actual LED position and the geometry model, found by the least square fitting method, are chosen for the 3-D triangulation. To directly get the rotation matrix and the translation vector of the probe coordinate system  $C_p$  with respect to the world coordinate system  $C_w$ , the origin of the geometry model is shifted and rotated into the origin of  $C_w$ . The coordinate systems are shown in Figure. 1. Thus, the rotation and translation of the actual LED position in relation to the model are the same as to the origin of  $C_w$ .

A similar procedure is carried out with the IR-LEDs of the calibration device. Subsequently the relative position and orientation of the TRUS probe coordinate system  $C_p$  with respect to the coordinate system  $C_c$ , defining the calibration device, is known.

To define the exact position of the image plane, defined by a coordinate system  $C_1$ , in relation to the probe coordinate system the probe has to be calibrated. To perform this calibration the probe is inserted into the water basin filled with distilled water as shown in Figure. 2. The calibration device is placed into the water basin at a position in which the probe image plane intersects the 3-D calibration pattern. The intersection points of the nylon strings and the image plane are displayed as bright spots in the image. These are interactively defined by the user and, because of the noise, with support of a displayed graphical pattern of the expected intersection point positions. Due to the non parallel arrangement of the strings, the 3-D positions of the intersection points can be calculated as published in [6].

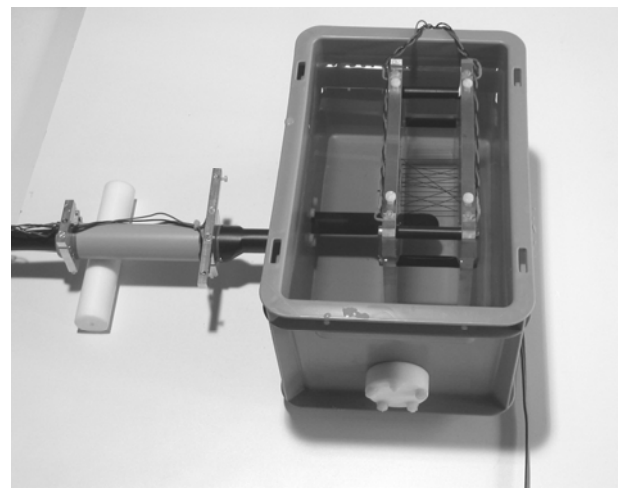


Figure 2: The calibration arrangement as used in this work. The calibration device is inserted into a water basin and sealed with an O-ring flange. The tracker is mounted on the TRUS probe.

In Figure. 3 the calibration pattern of one out of nine N-shaped structures and the intersecting ultrasound plane is presented. The points A, B, C and D are known in calibration device coordinates  $C_c$ . The coordinates of the intersecting points P, Q, R are unknown, because the

position of the ultrasound plane is unknown. The vector  $\vec{r}_C(Q)$  to the intersection point Q can be calculated by

$$\vec{r}_C(Q) = \vec{r}_C(B) + k \cdot (\vec{r}_C(C) - \vec{r}_C(B)) \quad (1)$$

where  $\vec{r}_C$  denotes vectors in calibration coordinate system showing to the points Q, B and C respectively.

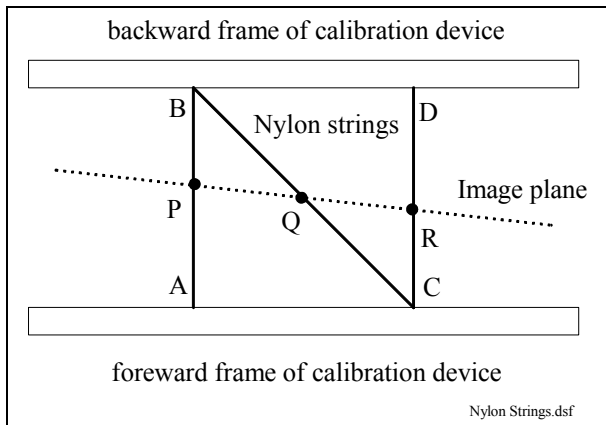


Figure 3: 3-D calibration pattern and the arrangement of N-shaped nylon strings which are clamped between the frame of the calibration device.

The nylon strings  $\overline{AB}$  and  $\overline{CD}$  are parallel. Consequently the triangles PBQ and QCR are similar.

$$k = \frac{\overline{BQ}}{\overline{BC}} = \frac{\overline{PQ}}{\overline{PR}} \quad (2)$$

is defined interactively in the image plane.

Now, the point set  $M_{i,C}$  of the intersection points of the not parallel nylon strings is determined. The first index I,  $i=1, \dots, 9$ , denotes the point number, the second one the coordinate system in use. The set is then transformed into  $C_W$  and hence into  $C_P$  with the help of the transformation matrices  $T_{P \leftarrow C}$  in which the indices denote the coordinate systems in direction of the transformation.

$$M_{i,P} = T_{P \leftarrow C} * M_{i,C} \quad (3)$$

$$\text{where } T_{P \leftarrow C} = T_{P \leftarrow W} * T_{W \leftarrow C} \quad (4)$$

Both transformations on the right hand side of (4) are defined by the navigation system.

With the help of a non iterative algorithm published in [9], based on quaternions, the rotation matrix  $R$  and translation vector  $\vec{t}$  of (5), which represent the calibration parameters, are determined in an over-defined equation system :

$$M_{i,P} \cong R \cdot M_{i,I} + \vec{t} \quad (5)$$

where  $\vec{t}$  represents a translation vector pointing from the origin of  $C_P$  to the origin of  $C_I$ .

The parameters minimize the square sum error:

$$F = \sum_{i=1}^{N=9} (R \cdot M_{i,I} + \vec{t} - M_{i,P})^2 = \text{MIN} \quad (6)$$

$N=9$  is the number of points used for one measurement.

An application was developed, which allows the calibration of the navigation system as well as the calibration of the TRUS probe as it is described above.

Assumed that the calibration processes have been performed, a set of US images with their corresponding parameters can be recorded and displayed. To perform the recording, the user moves the probe slowly along the  $x_P$ -axis. If the distance of the probe exceeds a defined interval of e. g. 2 mm to the last ultrasound image position recorded, the next image is acquired and stored with its position information. By this method it is possible to record 3-D US images [10].

## Measurements

13 Measurements were carried out according to the above described procedure. In the US image the set of nine intersection points  $M_{i,I}(x_{i,I}, y_{i,I})$  were defined interactively near the positions proposed by the graphical pattern. This 2-dimensional point set is used for (1) and (2) to get the 3-dimensional point set  $M_{i,C}(x_{i,C}, y_{i,C}, z_{i,C})$ .  $M_{i,C}$  is transformed according to (3) into a point set  $M_{i,P}$  defined in the TRUS probe coordinate system  $C_P$ .  $M_{i,I}$  and  $M_{i,P}$  are correlated by (5) from which the calibration parameters  $R$  and  $\vec{t}$  are calculated. Now the rotation matrix  $R$  and the translation vector  $\vec{t}$  between the origin of the image coordinate system and the US probe system respectively are known.

With the now known parameters  $R$  and  $\vec{t}$  of the position of the US image plane in coordinate system  $C_P$  and with the position of the calibration device the positions of the nine intersection points were calculated in  $C_I$ . The sum  $S$  of the Euclidean distances of the calculated points  $r_{n,C}$  and the interactively defined points  $r_{n,I}$  during measurement is calculated and taken as a measure of the preciseness of the calibration process.

$$S = \frac{1}{N} \sum_{n=1}^N \sqrt{r_{c,n}^2 - r_{i,n}^2} \quad (7)$$

Measurements in which the average of the sum of Euclidean distances  $S$  was larger than 2mm were treated as resulting from a not proper definition of calibrating points and were omitted in the mean calculation. This was the case in four out of the 13 measurements undertaken. The remaining results are shown in Table 1.

Table 1: Calibration measurements

Measurement	$\alpha/^\circ$	$\beta/^\circ$	$\gamma/^\circ$	S/mm
1	91.48	0.47	88.30	1.36
2	91.12	1.24	90.47	1.93
3	90.49	0.29	82.55	1.42
4	91.16	0.96	89.34	1.61
5	88.02	0.63	88.93	1.25
6	91.41	1.19	89.78	1.63
7	90.23	1.01	87.59	1.72
8	91.47	0.64	86.23	1.40
9	91.36	0.89	90.74	1.92
Average	90.75	0.81	88.21	1.58
Standard deviation	1.05	0.31	2.41	0.23

### Discussion

The measurements show a good coincidence of the US image plane with its assumed position. Expected values are  $\alpha = 90^\circ$  and  $\gamma = 90^\circ$ , which for small values describe the angles between the image plane and the z-axis of the probe. The angle  $\beta$  is of no relevance in this paper, because it describes the rotation of the image plane due to the  $x_p$ -axis which is defined by the mounted tracking system of the probe. Taking into account the standard image width of 78.4 mm and height of 64.0 mm a value of  $\Delta\alpha = 1^\circ$  results in a deviation of the image plane at the utmost corner with respect to the probe's x-axis of 0.52 mm and  $\Delta\gamma = 1^\circ$  such of 0.68 mm respectively. Both deviations sum up to approximately 1 mm. These values have to be related with the slice thickness of the US image which until now has not been considered.

### Conclusions

As discussed in [11], the former application of an electro-magnetic navigation system used in [12] did not result in a satisfactory accuracy, because of the interference with the ferromagnetic environment in an operating room. The system developed in this thesis is based on optical localization technology which is insensitive to metallic objects. The significant accuracy for medical use of  $\pm 1$ mm could be achieved in a volume that is accurate enough for the use in interstitial transperineal brachytherapy for prostate carcinoma. Before using the camera system in operating rooms, it should be installed and calibrated in a way that the center of the calibration pattern is located where the TRUS probe is moved to, when the US images show the center of the prostate. At this position, the highest accuracy of the camera system has been measured. Because the main movement of the probe mounted on a stepper is at the same z-level and only in x-direction, the accuracy of 0.22mm RMS for navigation at calibration level is most relevant.

The deviation caused by the non proper alignment of the image plane is with approximately  $\pm 1$ mm larger

than the navigational inaccuracy. Thus the TRUS probe used should be calibrated and the parameters included into the calculation for navigation.

### Acknowledgements

We thank B-K Medical Medizinische Systeme GmbH in 25451 Quickborn, Germany, for putting a US-scanner at our disposal for this work.

### References

- [1] VOSS H.: 'Development of a Stereo-Optical 3-D Navigation System for Ultrasound-Guided Brachytherapy for Prostate Carcinoma', Diploma thesis, Department of Computer Science, University of Applied Sciences of Wiesbaden, 2005.
- [2] HARM M.: 'Entwicklung eines dreidimensionalen Nadelpositionierungssystems zur Strahlentherapie', Diploma thesis, Department of Computer Science, University of Applied Sciences of Wiesbaden, 2000.
- [3] RICHTER D., STRASSMANN G., HARM M.: 'Ein dreidimensionales Sondennavigationssystem für die extra-kranielle Brachytherapie in der Strahlentherapie', Bildverarbeitung für die Medizin 2001, Springer; pp. 44-48, 2001.
- [4] PAGOULATOS N., HAYNOR D. R., YONGMIN K.: 'A fast calibration method for 3-D tracking of ultrasound images using a spatial localizer', Ultrasound in Med. & Biol., Vol. 27, No. 9, pp. 1219-1229, 2001.
- [5] BOUCHET L. G., MEEKS S. L., GOODCHILD G., BOVA F. J., BUATTI J. M. AND FRIEDMAN W. A. (2001): 'Calibration of three-dimensional ultrasound images for image-guided radiation therapy', *Physics in Medicine and Biology*, 46(2), pp 559-577
- [6] LINDSETH F., TANGEN G.A., LANGØ TH., BANG J.: 'Probe calibration for freehand 3-D ultrasound', *Ultra-sound in Med. & Biol.*, 29(11), pp. 1607-1623, 2003.
- [7] TSAI R., 'An Efficient and Accurate Camera Calibration Technique': *Computer Vision and Pattern Recognition IEEE*, Miami Beach, 1986.
- [8] POSCH S.: 'Automatische Tiefenbestimmung aus Grauwertbildern', Deutscher Universitätsverlag, Wiesbaden, 1990.
- [9] HORN, B. K. P.: 'Closed-form solution of absolute orientation using unit quaternions'. *Journal of the Optical Society of America A*,4(4), pp. 629-642, 1987.

- [10] BERTHOLD K.: 'Kalibrierung und Visualisierung von 3-D Positionsdaten mit bildgebenden US Sensoren', Diploma thesis, Department of Computer Science, University of Applied Sciences of Wiesbaden, 2005.
- [11] BALE R. J., SWEENEY R. A., LUKAS P.: 'Comment on: G. Straßmann et al. : Accuracy of 3-D Needle Navigation in Interstitial Brachytherapy in Various Body Regions, (and Reply to Comment)', *Strahlen-therapie und Onkologie*, 178(11), pp. 648–650, 2002.
- [12] STRABMANN G., KOLOTAS C., HEYD R., WALTER S., BALTAS D., MARTIN T., VOGT H., IOANNIDIS G., SAKAS G., ZAMBOGLOU N.: 'Navigation system for interstitial brachytherapy', *Radiotherapy and Oncology*, 56:49–57, 2000.